https://doi.org/10.48048/tis.2024.8329

Fabrication of Nanofiber Membranes from Waste-Expanded Polystyrene (EPS) Combined with Zinc Oxide Nanoparticles (ZnO NPs) and its Photocatalytic Activity

Yulianto Agung Rezeki[1], Lia Dwi Setyaningsih[1], Hanifah Setyaning Budi[1], Julia Angel[2], Muhammad Fahroji[3], Ratih Amalia[3], Bagas Haqi Arrosyid[3], Gugus Handika[3], Kurniawan Eko Saputro[3], Alfian Noviyanto[3,4] and Akmal Zulfi[5,*]

[1]Department of Physics Education, Universitas Sebelas Maret, Surakarta 57126, Indonesia
[2]Research Center for Nanotechnology System, National Research and Innovation Agency (BRIN), Banten 15314, Indonesia
[3]Nano Center Indonesia, Banten 15314, Indonesia
[4]Department of Mechanical Engineering, Mercu Buana University, Jakarta 11650, Indonesia
[5]Research Center for Environmental and Clean Technology, National Research and Innovation Agency (BRIN), Bandung 40135, Indonesia

(Corresponding author's e-mail: e-mail: akmal.zulfi.m@brin.go.id)

Received: 20 April 2024, Revised: 26 May 2024, Accepted: 2 June 2024, Published: 1 October 2024

Abstract

Society must face the challenge of creating high-value products from recycled waste polymers. This research focuses on the synthesis of nanofiber membranes from waste-expanded polystyrene (EPS) using electrospinning. Zinc oxide nanoparticles (ZnO NPs) enhance the photocatalytic activity of the fiber membrane. ZnO is a more useful alternative to TiO_2 as a form of photocatalyst for degrading contaminants in water. This study systematically investigated the effects of varying amounts of ZnO NPs on fiber membrane nanostructure and photocatalytic activity. Methylene blue was used to measure the photocatalytic efficiency of fiber membranes, as they are commonly used in textile wastewater and exposed to ultraviolet light for 20 h. The results showed that the fiber membrane containing ZnO NPs with a concentration of 1 % effectively degraded methylene blue.

Keywords: Waste-Expanded polystyrene, Zinc oxide nanoparticles, Nanofiber, Electrospinning, Photocatalytic activity

Introduction

One of the 5 major plastics based on petroleum, polystyrene (PS) is a plastic that is commonly utilized in a variety of applications, such as disposable products in commodity packaging, food packaging, and building materials, its Society for Plastic Industry (SPI) number is 6, which indicates the challenge of recycling it [1,2]. Compared to the other types of PS, such as high impact polystyrene (HIPS) and oriented polystyrene (OPS), expanded polystyrene (EPS) is a type of stable polymer foam in the oldest category of bead foam polymer materials with a very low density because it consists of separate air cavities in the polymer matrix [3]. EPS is often found in EPS handicrafts, food packaging, instant noodle cups, and electronic packaging. Due to its low density, it is difficult for EPS to decompose in the environment, which makes it easily spread by the wind and becomes a real nuisance in polluting the environment, thereby

endangering human and animal life [4,5]. Along with increasing pollution problems in this environment, the demand for recycling processes has increased to convert waste into high-value products. In recycling EPS, because of its density, it can cause worse problems that increase transportation and disposal costs, making it more expensive and not feasible [6]. Nowadays, there are 4 main types of polymer recycling: Quaternary recycling, chemical recycling, and direct recycling (primary and secondary recycling) [7,8].

So far, several researchers have carried out chemical recycling with dissolving waste EPS in a solvent such as dimethylformamide (DMF) using the electrospinning method [9-11]. Electrospinning is one of the simple and affordable processes [12-15] that uses high voltage to generate charges on the surface of the polymer solution to make fibers with a very large surface area-to-volume ratio from precursor solutions [13,16]. By converting this EPS waste into fibers in nanofibers, it was proven to be an efficient heterogeneous photocatalyst as a supporting matrix for catalytic metal nanoparticles [17]. In 2015, Rajak *et al*. successfully fabricated EPS nanofiber containing TiO_2 nanoparticles as a photocatalytic agent for degrading wastewater. In this study, the photocatalyst agent was zinc oxide nanoparticles (ZnO NPs). ZnO is being thoroughly investigated as a more useful alternative to TiO_2 as a form of photocatalyst due to its extremely high bandgap (3.37 eV) and significant light absorption within the UV region of the optical spectrum [18]. ZnO is a feasible substitute photocatalyst for water treatment operations since it is more economical and efficient than TiO_2 [19]. Nanofibers that contain ZnO NPs also prevent any nanoparticles from being wasted in their application as photocatalysts [20].

This study aimed to enhance the photocatalytic activity on EPS/ZnO nanofiber membranes. To our knowledge, the research on combining waste EPS-based polymer materials with a photocatalytic agent ZnO NPs strategy has not yet been reported. The structure of the prepared nanofiber was characterized using scanning electron microscopy (SEM), Fourier transform infrared (FTIR) spectroscopy, and Raman Spectroscopy. The photocatalytic activities of EPS/ZnO nanofiber were investigated by perceiving the degradation of methylene blue. Experimental results have demonstrated that the EPS/ZnO nanofiber was simultaneously efficient as a photocatalyst agent. These findings may offer potential applications in the field of photocatalysis.

Materials and methods

Materials

Waste EPS used in this study was from electronic packaging. Commercial ZnO NPs (average particle size of 100 nm), methylene blue (MB), and dimethylformamide ($(CH_3)_2NC(O)H$, DMF) were used in this study.

Preparation of EPS/ZnO fiber membranes

Before preparation solutions, the waste EPS was thoroughly washed with distilled water, followed by drying at room temperature. After that, the waste EPS was cut into small pieces (the size approximately 1.5 cm in length).

Table 1 The ratio of zinc oxide (ZnO) NPs in EPS solution.

Mixing ratio (g)		ZnO NPs in EPS solution (wt. %)	Sample name
EPS solution	ZnO NPs		
5	0	0	EPS
5	0.005	0.1	EPS/ZnO 0.1 %
5	0.025	0.5	EPS/ZnO 0.5 %
5	0.05	1	EPS/ZnO 1 %

For the preparation of EPS/ZnO solution, 15 wt. % EPS solutions were provided by dissolving 0.75 g of EPS in 4.25 mL DMF for 30 min at room temperature. After a homogeneous precursor solution was obtained, different amounts of ZnO NPs (0.1, 0.5, 1 wt. %) were added to the EPS solution. The variations of ZnO NPs concentration in EPS solution are shown in **Table 1**. The solution was stirred at 45 °C for 1 h until it became completely homogeneous. Next, the precursor solutions were processed using an electrospinning technique to obtain EPS/ZnO nanofiber membranes.

Electrospinning process

Electrospinning (ILMI-N101) was used to prepare the fiber. The electrospinning equipment was equipped with an aluminum collection plate, a high-voltage power source, a syringe, and a needle with an internal diameter of 0.84 mm for creating the EPS/ZnO nanofibers. The syringe was attached to a syringe pump to regulate the flow rate. The EPS/ZnO solution was electrospun at a high voltage of 12 kV with a needle tip-to-collector distance of 10 cm and a solution flow rate of 0.7 mL/h. Electrospinning was carried out continuously for 2 h at a temperature of 25 °C and relative humidity of 60 % to synthesize nanofibers.

Characterization of EPS/ZnO fiber membranes

The fiber diameter and morphologies of the fabricated EPS nanofiber membranes were investigated using a scanning electron microscope (SEM) (JEOL, JSM-6510LV). ImageJ software was used to analyze the collected SEM micrographs to calculate the average fiber diameters and perform statistical analysis. The diameter of the fibers was calculated by counting 100 points across each fiber in the SEM picture. The uniformity of fibers was determined by calculating the coefficient of variation (CV) equation using Eq. (1):

$$CV = \frac{\sigma}{\mu} \quad (1)$$

where σ is the standard deviation and μ is the average diameter of fibers [13]. When the CV value was less than 0.3, it represented uniform nanofibers; when it was greater than 0.3, it represented nonuniform nanofibers [21]. In addition, an Energy Dispersive X-ray (EDX) was used to observe the distribution of ZnO NPs in the electrospun nanofibers.

The FTIR (Thermo Fisher Scientific, NICOLET IS10) analysis was performed to determine the existing functional groups in EPS nanofiber, ZnO NPs, and EPS/ZnO nanofibers at the wavenumber of 3,500 to 400 cm^{-1}. Their peak numbers may identify the usual functional groupings in each sample. Along with gathering data on each compound's purity, it is also possible to acquire information on each compound's structure.

Raman spectroscopy (Thermo Fisher, DXR3xi) was used to analyze molecular vibrations in materials. Raman peaks' locations are frequently linked to certain chemical group motions. The integral of the Raman line is proportional to the number of stimulated vibrations, and the breadth of the Raman line vibrations reflects interactions between these vibrations [22]. The laser diode's output has been set at 5.0 MW, and the accumulations have been raised to 1,000. The splitting of Raman bands was seen over the whole spectrum to obtain significant noise to emerge in the spectra.

Photocatalytic activity

Photocatalytic properties of EPS/ZnO are related to the membrane's ability in dye degradation. Photocatalytic activities of EPS/ZnO nanofiber were investigated by perceiving methylene blue (MB) degradation under UVA light. The degradation of MB solution under UV light irradiation was used to measure the photocatalytic efficiency of electrospun nanofiber EPS/ZnO. In the experiment, an electrospun nanofiber EPS/ZnO sample of 0.014 g was added to a 5 mL 20 ppm MB solution. The UV light was used for irradiation. A double-beam UV-Vis spectrophotometer measured The degraded MB concentration (Labtron LUS-B13 series number M18P21090201). The absorbance of the suspension was measured at λ_{max}= 585 nm. The degradation efficiency was evaluated by using the following equation [23]. MB degradation = $(C_0 - C)/C_0$. Where C_0 is the initial concentration of MB, and *C* is the remaining concentration of MB after UV irradiation for time *t*.

Results and discussion

Morphology of the electrospun EPS/ZnO fiber membranes

The EPS/ZnO nanofibers were obtained with smooth, uniform, and beadless morphology with an average diameter of 600 - 800 nm (Error! Reference source not found). The average diameters of obtained nanofibers were 614, 482, 663, and 805 nm for the ZnO NPs concentrations of 0, 0.1, 0.5, and 1 wt. % , respectively, as shown in **Figure 1**. The coefficient of variation (CV) of the nanofiber membranes obtained values below 0.3 for each membrane, indicating that each nanofiber membrane's morphology is uniform [24].

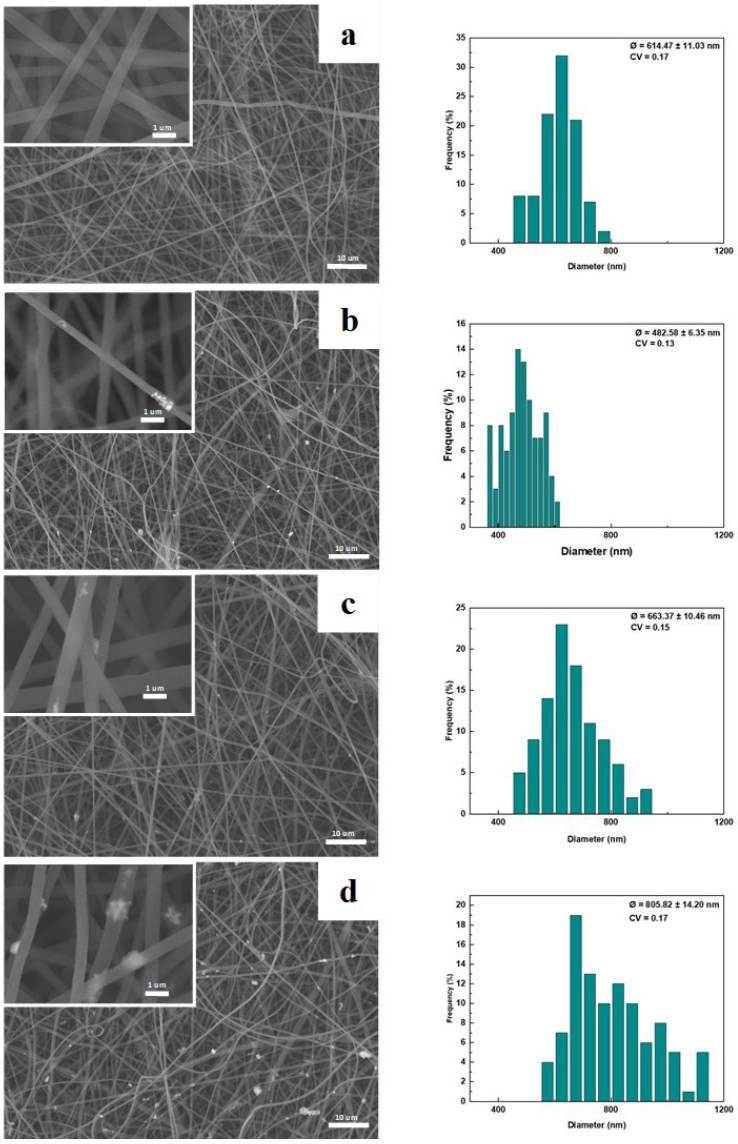

Figure 1 SEM micrographs of the electrospun nanofiber (a) EPS, (b) EPS/ZnO 0.1 % , (c) EPS/ZnO 0.5 %, and (d) EPS/ZnO 1 % , including the average fiber diameter and its distribution.

The effects of various concentrations of ZnO NPs were also investigated in this work. As can be seen in the SEM images, the ZnO NPs were successfully encapsulated in the EPS matrix. As ZnO NPs concentration increased, the average diameter size of the nanofiber membranes also increased. The higher the ZnO NPs concentration, the more ZnO NPs can be encapsulated in the EPS matrix. When ZnO NPs was added, the diameter of electrospun nanofibers was slightly decreased. This is because adding ZnO NPs causes the solution to become more conductive than the pure EPS solution. Additionally, as the ZnO NPs concentrations increases, the electrospun nanofiber's diameter correlates with its viscosity [17]. The presence of nanoparticles increases the diameter of polymer nanofibers during electrospinning and the increase in diameter leads to a decrease in the surface-to-volume ratio of the material [20]. Further characterization using EDX was carried out to confirm the presence of ZnO NPs in the electrospun nanofiber.

To further confirm the composition and distribution of elements in electrospun EPS/ZnO nanofibers, the samples' EDX spectrum and EDX mapping were analyzed. As shown in **Table 2**, in the EDX spectrum,

the C, Zn, and O elements all existed in the sample of EPS/ZnO. The expanded polystyrene is characterized by the major chemical compositions of Carbon (C). The element Al is also visible in the EDX spectrum of electrospun EPS/ZnO nanofiber because during EDX characterization, the sample substrate, aluminum, was included. Moreover, the C, Zn, and O elements are not distributed regularly and uniformly because they are still agglomerated in some areas [25]. As the concentration of ZnO NPs increases, the amount of Zn and O detected increases.

Table 2 EDX spectrum and EDX mapping images of the electrospun EPS/ZnO nanofiber.

EDX spectrum		**EDX mapping**		
		C	**Zn**	**O**
EPS	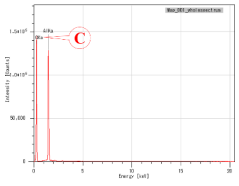	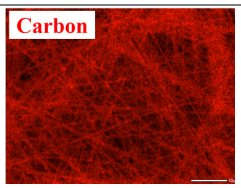	-	-
EPS/ZnO 0.1 %	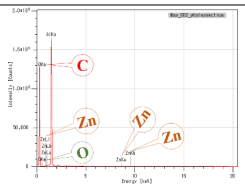	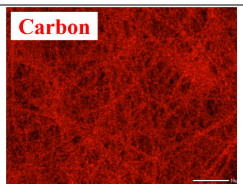	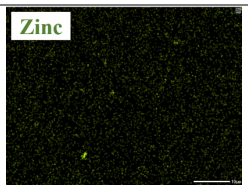	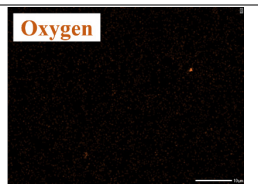
EPS/ZnO 0.5 %	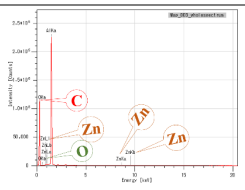	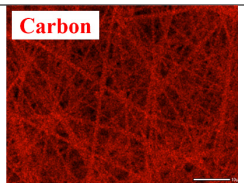	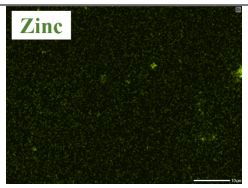	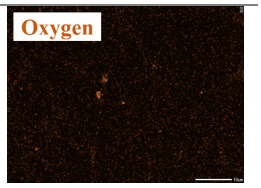
EPS/ZnO 1 %	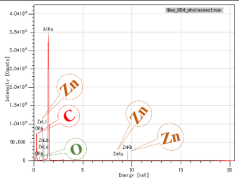	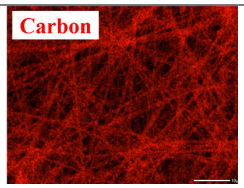	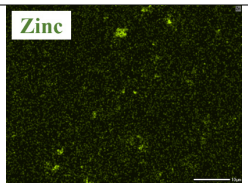	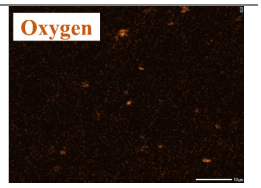

FTIR characteristic of the electrospun EPS/ZnO fiber membranes

The FTIR spectra are shown in **Figure 2**. The FTIR range of EPS from 3,100 to 3,000 cm^{-1} represents the C-H aromatic stretching vibration of the benzene ring. The peaks at 2,924 and 3,024 cm^{-1} demonstrate the asymmetric and symmetric stretching vibrations CH_2. Other characteristic peaks were observed in the 1,658 - 1,456 cm^{-1} range, attributed to the C = C bond stretching vibration of the benzene ring [26]. The peaks at 900 - 600 cm^{-1} were attributed to C-H out-of-plane bending vibration, and specifically those at 752, 696, and 538 cm^{-1} were attributed to C-H deformation vibration of the monosubstituted benzene ring [11]. The FTIR characteristic peaks of DMF were 1,673, 1,389, 1,256, and 1,096 cm^{-1} [10]. Those peaks were not present in the FTIR spectra of the EPS/ZnO nanofiber mats. The peak of ZnO in the transmittance peak at 430 cm^{-1} refers to the stretching vibration bond of Zn-O [18].

The resulting spectra of electrospun EPS/ZnO 0.1 %, EPS/ZnO 0.5 % , and EPS/ZnO 1 % show no difference compared to the spectra of electrospun pure EPS mats, which implies that the incorporation of different concentrations of ZnO NPs does not affect the generation of extra peaks in the EPS spectra. However, with the increase of ZnO NPs content, the intensity of the characteristic peaks was weakened

accordingly. This demonstrates that ZnO NPs was successfully incorporated into the nanofiber. The characteristics of ZnO at peaks 430 cm^{-1} were seen in EPS/ZnO nanofibers with a ZnO NPs concentration of 1 wt. % but were not seen significantly at ZnO NPs concentrations of 0.1 and 0.5 wt. % . Therefore, the interaction between ZnO NPs embedded in the EPS matrix is more likely physical than chemical [18].

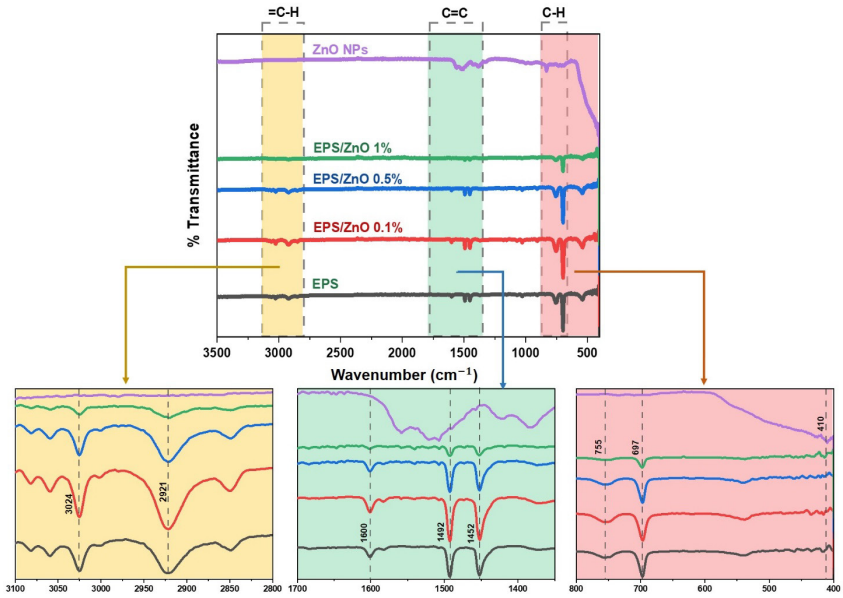

Figure 2 FTIR spectra of the electrospun EPS/ZnO nanofiber membranes.

Raman characteristic of the electrospun EPS/ZnO fiber membranes

Raman spectroscopy is a potent tool for analyzing the molecular vibrations in materials [22]. Compared to FTIR, Raman spectroscopy can more specifically analyze the peaks of ZnO NPs because ZnO is a metal nanoparticle whose spectra are often found at Raman shifts below 500 cm^{-1} [27]. Raman peaks tend to correspond with particular chemical group motions. The Raman spectra of EPS/ZnO nanofibers are seen in **Figure 3**, indicating the superposition between the lines caused by the polymeric matrix (EPS) and the filler (ZnO NPs). **Figure 3** shows that the Raman lines of the polymeric matrix are rapidly broadened and weaker as the concentration of the ZnO NPs is increased.

EPS has an intense v(CC) aromatic carbon-carbon bond and (CC) carbon-carbon stretch at 1,001 and 1,155 $cm^{-1,}$ respectively [28]. Peaks at 1,031 cm^{-1} are assigned to C-H bending, and peaks at 1,602 cm^{-1} modes are the most intense band corresponding to the C=C aromatic ring stretching [26]. The characteristic ZnO peaks were observed in the Raman spectrum at 99, 205, 273, 331, 436, and 532 cm^{-1}. The observed peaks at 99 and 436 cm^{-1} are assigned to E_2(low) and E_2(high) modes, respectively. E_2 mode consists of low and high basic phonons modes representing wurtzite structure of good crystalline quality [29,30]. These are typical for the Raman active branches, attributed to the ZnO nonpolar optical phonons [31,32]. The broad peaks around 273 and 532 cm^{-1} are assigned to silent B_1(low) and B_1(high) modes, respectively, which became activated by inducting defects [27]. Peaks at 205 and 331 cm^{-1} can be assigned to the second-order Raman spectrum arising from zone-boundary phonons 2TA (M) and $2E_2$ (M), respectively [33]. The peaks of the characteristics of ZnO were seen in EPS/ZnO nanofibers with a ZnO concentration of 1 wt. % but were not seen significantly at ZnO NPs concentrations of 0.1 and 0.5 wt. % .

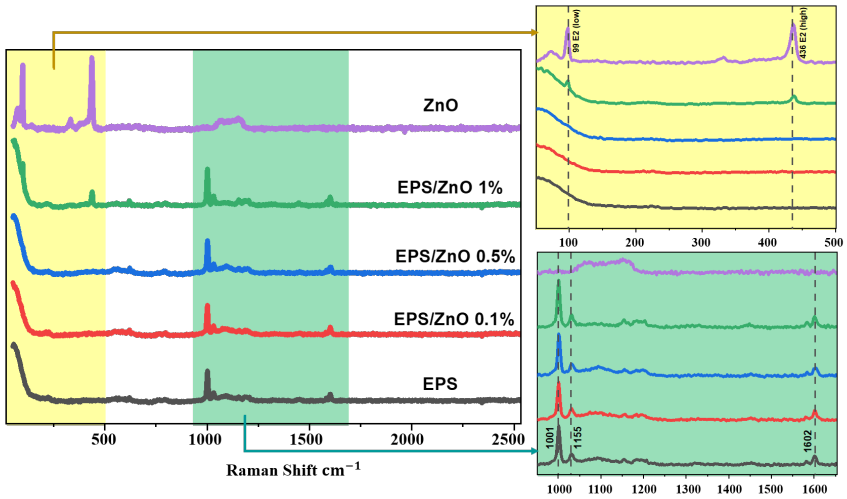

Figure 3 Raman spectra of the electrospun EPS/ZnO nanofiber membranes.

Photocatalytic activity

The photocatalytic activity of electrospun nanofiber EPS/ZnO in MB solution was evaluated by photodegradation of MB. The degradation efficiency was evaluated by using the following equation [23].

MB degradation = $(C_0 - C)/C_0$

C_0 is the initial concentration of MB, and C is the remaining concentration of MB after UV irradiation for time t. The results are indicated in **Table 3**. As a result, electrospun nanofiber EPS/ZnO 1 % shows the highest efficiency. The 45 % of MB was degraded within 20 h of irradiation. However, EPS/ZnO 0.1 and 0.5 % yielded rather lower efficiency than without ZnO NPs. Electrospun nanofiber EPS without ZnO NPs exhibited only 3 % efficiency and samples containing 0.1 and 0.5 wt. % ZnO showed 4 and 16.5 %, respectively. **Figure 4** shows the evolution of absorbance as a function of time, photocatalytic degradation of MB under UVA light irradiation, first-order reaction kinetic curves for the MB degradation reaction, and the % degradation of MB.

Table 3 Degradation of Methylene Blue under UV Light after 20 h on an Electrospun EPS/ZnO Nanofiber Membranes.

No	Samples	MB initial concentration (ppm)	MB final concentration (ppm)	% MB degradation = $(C_0 - C)/C_0$
1	EPS	20.0	19.4	3
2	EPS/ZnO 0.1 %		19.2	4
3	EPS/ZnO 0.5 %		16.7	16.5
4	EPS/ZnO 1 %		11.0	45

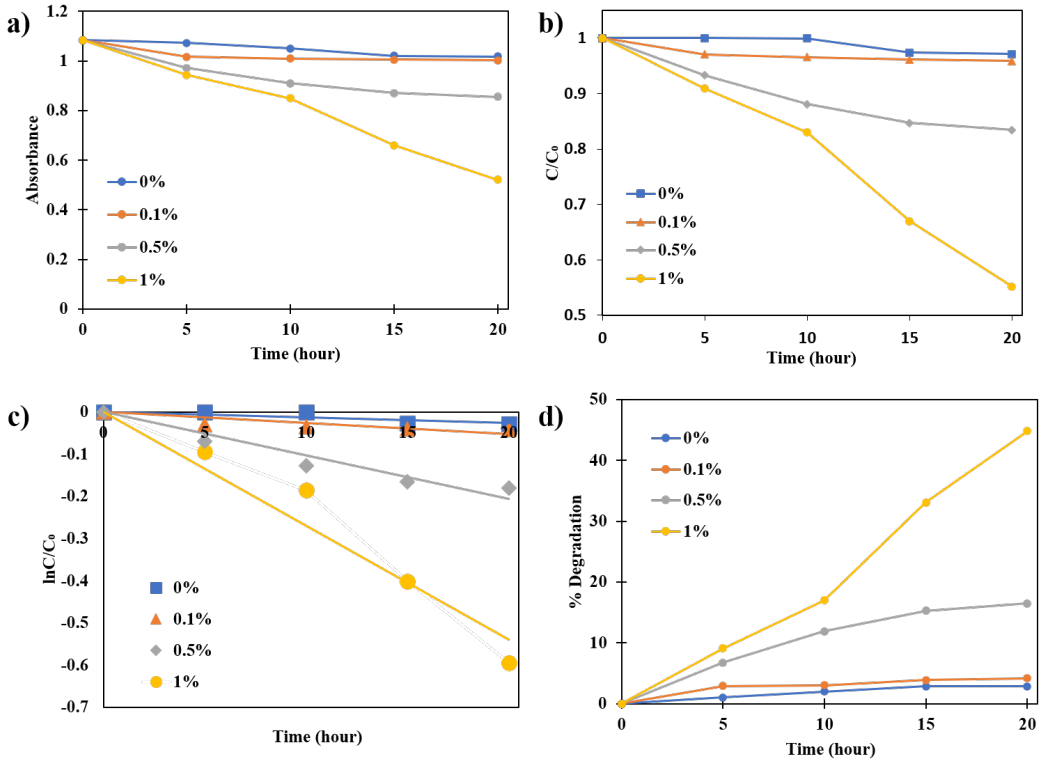

Figure 4 a) The evolution of absorbance as a function of time. b) Photocatalytic degradation of MB under UVA light irradiation. c) First-order reaction kinetic curves for the MB degradation reaction. d) The % degradation of MB.

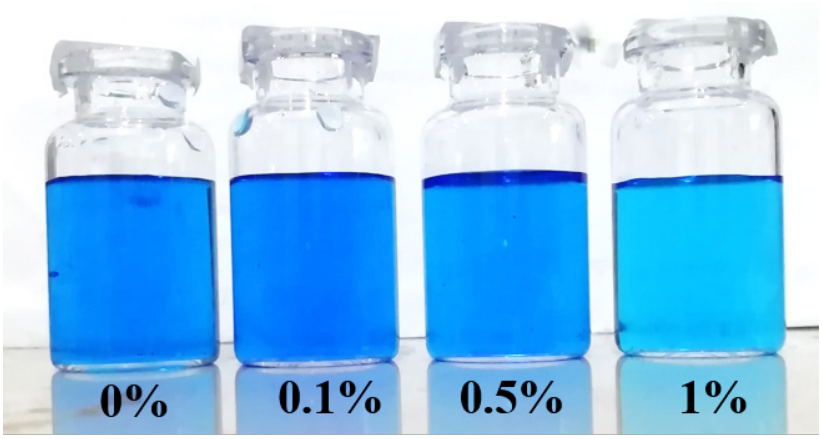

Figure 5 Degradation color of MB after 20 h.

The study found that the concentration of ZnO used was too small to have an efficient photocatalytic effect on methylene blue color degradation. The degradation color of MB after 20 h is shown in **Figure 5**. A larger concentration of ZnO is needed to improve the nanofiber membrane's photocatalytic ability. It has been found that excessive amounts of ZnO NPs in the membrane can lead to the membrane becoming brittle [9]. Therefore, it is necessary to identify the appropriate composition for the photocatalyst membrane to ensure it is effective and efficient in removing organic contamination during its application.

Conclusions

The authors successfully transformed EPS waste into a valuable product through electrospinning, resulting in a material with photocatalytic properties. Analysis of the FTIR spectrum confirms the presence of ZnO in EPS/ZnO composite fibers, detectable at a wavelength of 430 cm^{-1}. However, this presence is only observable at 1 wt. % , remaining undetectable at concentrations of 0.1 and 0.5 wt. % . This result is reinforced by Raman spectra, which show the presence of ZnO at the Raman shifts of 99 and 436 cm^{-1} at 1 wt. % , without being detected at concentrations of 0.1 and 0.5 wt. %. From this, we can conclude that the interaction between ZnO NPs and the EPS matrix is more likely physical than chemical. In addition, our photocatalytic testing has shown that the ZnO-containing fiber membranes are effective at breaking down methylene blue, indicating the EPS/ZnO composite nanofibers' ability to remove organic contaminants.

Acknowledgments

The authors thank Nano Center Indonesia and E-SMART Research Group for providing laboratory facilities and National Research and Innovation Agency (BRIN) through the Research and Innovation for Advanced Indonesia (RIIM) Grant (Grant No.12/II.7/HK/2023) for financial support.

References

[1] N Chaukura, W Gwenzi, T Bunhu, DT Ruziwa and I Pumure. Potential uses and value-added products derived from waste polystyrene in developing countries: A review. *Resour. Conserv. Recycl.* 2016; **107**, 157-65.

[2] C Wang, Q Wang, J Yu, X Wang, L Wang, B Zhao, L Hin, W Liu, Z Wang, H Chen and Q Wu. Converting waste expanded polystyrene into higher-value-added hyper-crosslinked porous polymer for rapid and high-efficient adsorption of aflatoxins. *J. Clean. Prod.* 2023; **408**, 137102.

[3] L Prasittisopin, P Termkhajornkit and YH Kim. Review of concrete with expanded polystyrene (EPS): Performance and environmental aspects. *J. Clean. Prod.* 2022; **366**, 132919.

[4] M Liu, Z Xie, H Ye, W li, W Shi, Y Liu and Y Zhang . Waste polystyrene foam-chitosan composite materials as high-efficient scavenger for the anionic dyes. *Colloids Surf. A* 2021; **627**, 127155.

[5] PI Morgado, A Aguiar-Ricardo and IJ Correia. Asymmetric membranes as ideal wound dressings: An overview on production methods, structure, properties and performance relationship. *J. Membr. Sci.* 2015; **490**, 139-51.

[6] GD Mumbach, A Bolzan and RAF Machado. A closed-loop process design for recycling expanded polystyrene waste by dissolution and polymerization. *Polymer* 2020; **209**, 122940.

[7] RF Cella, GD Mumbach, KL Andrade, P Oliveira, C Marangoni, A Bolzan, S Bernard and RAF Machado. Polystyrene recycling processes by dissolution in ethyl acetate. *J. Appl. Polym. Sci.* 2018; **135**, 46208.

[8] SM Al-Salem, P Lettieri and J Baeyens. Recycling and recovery routes of plastic solid waste (PSW): A review. *Waste Manag.* 2009; **29**, 2625-43.

[9] A Rajak, MM Munir, A Mikrajuddin and K Khairurrijal. Photocatalytic activities of electrospun TiO2/styrofoam composite nanofiber membrane in degradation of waste water. *Mater. Sci. Forum*. 2015; **827**, 7-12.

[10] A Rajak, DA Hapidin, F Iskandar, MM Munir and K Khairurrijal. Electrospun nanofiber from various source of expanded polystyrene (EPS) waste and their characterization as potential air filter media. *Waste Manag.* 2020; **103**, 76-86.

[11] BH Arrosyid, A Zulfi, S Nur'aini, S Harrtati, AF Rafryanto, A Novviyanto, DA Hapidin, D Feriyanto

and K Khairurrijal. High-Efficiency water filtration by electrospun expanded polystyrene waste nanofibers. *ACS Omega* 2023; **8**, 23664-672.

[12] D Mustikasari, YA Rezeki, MM Munir, H Rachmawati and K Khairurrijal. Turmeric extract-loaded polyvinylpyrrolidone spherical submicron particles produced using electrohydrodynamic atomization: their physico-chemical properties and antioxidant activity. *Mater. Res. Express* 2019; **6**, 085415.

[13] G Prahasti, D Edikresnha, YA Rezeki, MM Munir and K Khairurrijal. The synthesis and characterization of composite electrospun fibers of polyvinylpyrrolidone and shell extract of melinjo (*Gnetum gnemon* L.). *Mater. Today Proc.* 2019; **13**, 187-92.

[14] YA Rezeki, DA Hapidin, H Rachmawati, MM Munir and K Khairurrijal. Formation of electrosprayed composite nanoparticles from polyvinylpyrrolidone/mangosteen pericarp extract. *Adv. Powder Tech.* 2020; **31**, 1811-24.

[15] YA Rezeki, N Wahyuni, MM Munir and K Khairurrijal. Synthesis of polyvinylpyrrolidone/mangosteen pericarp extract (MPE) fibered particles using electrospray. *J. Phys. Conf. Ser.* 2019; **1282**, 012033.

[16] A Zulfi, YA Rezeki, D Edikresnha, MM Munir and K Khairurrijal. Synthesis of fibers and particles from polyvinyl chloride (PVC) waste using electrospinning. *IOP Conf. Ser. Mater. Sci. Eng.* 2018; **367**, 012014.

[17] L Wang, J Ali, C Zhang, G Mailhot and G Pan. Simultaneously enhanced photocatalytic and antibacterial activities of TiO2/Ag composite nanofibers for wastewater purification. *J. Environ. Chem. Eng.* 2020; **8**, 102104.

[18] MM Abdel-Mottaleb, A Khalil, SA Karim, TA Osman and A Khattab. High performance of PAN/GO-ZnO composite nanofibers for photocatalytic degradation under visible irradiation. *J. Mech. Behav. Biomed. Mater.* 2019; **96**, 118-24.

[19] S O'Neill, JMC Robertson, V Hequet, F Chazarenc, X Pang, K Palphs, N Skillen and PKJ Pobertson. Comparison of titanium dioxide and zinc oxide photocatalysts for the inactivation of escherichia coli in water using slurry and rotating-disk photocatalytic reactors. *Ind. Eng. Chem. Res.* 2023; **62**, 18952-9.

[20] HR Pant, DR Pandeya, KT Nam, W Baek, ST Hong and HY Kim. Photocatalytic and antibacterial properties of a TiO2/nylon-6 electrospun nanocomposite mat containing silver nanoparticles. *J. Hazard. Mater.* 2011; **189**, 465-71.

[21] S Hartati, A Zulfi, PYD Maulida, A Yudhowijoyo, M Dioktyanto, KE Saputro, A Noviyanto and NT Rochman. Synthesis of electrospun PAN/TiO2/Ag nanofibers membrane as potential air filtration media with photocatalytic activity. *ACS Omega* 2022; **7**, 10516-25.

[22] DM Chipara, J Macossay, AVR Ybarra, AC Chipara, TM Eubanks and M Chipara. Raman spectroscopy of polystyrene nanofibers – Multiwalled carbon nanotubes composites. *Appl. Surf. Sci.* 2013; **275**, 23-7.

[23] J Yoon and SG Oh. Synthesis of amine modified ZnO nanoparticles and their photocatalytic activities in micellar solutions under UV irradiation. *J. Ind. Eng. Chem.* 2021; **96**, 390-6.

[24] A Zulfi, S Hartati, S Nur'aini, A Noviyanto and M Nasir. Electrospun nanofibers from waste polyvinyl chloride loaded silver and titanium dioxide for water treatment applications. *ACS Omega* 2023; **8**, 23622-32.

[25] D Gao, P Zhao, B Lyu, Y Li, Y Hou and J Ma. Carbon quantum dots decorated on ZnO nanoparticles: An efficient visible-light responsive antibacterial agents. *Appl. Organomet. Chem.* 2020; **34**, e5665.

[26] JA Yabagi, MI Kimpa, MN Muhammad, SB Rashid, E Zaidi and MA Agam. The effect of gamma

irradiation on chemical, morphology and optical properties of polystyrene nanosphere at various exposure time. *IOP Conf. Ser. Mater. Sci. Eng.* 2018; **298**, 012004.

[27] A Calzolari and MB Nardelli. Dielectric properties and raman spectra of ZnO from a first principles finite-differences/finite-fields approach. *Sci. Rep.* 2013; **3**, 2999.

[28] Y Fan and CJ Cornelius. Raman spectroscopic and gas transport study of a pentablock ionomer complexed with metal ions and its relationship to physical properties. *J. Mater. Sci.* 2012; **48**, 1153-61.

[29] Z Yao, K Tang, Z Xu, J Ye, S Zhu and S Gu. The luminescent inhomogeneity and the distribution of zinc vacancy-related acceptor-like defects in N-Doped ZnO microrods. *Nanoscale Res. Lett.* 2016; **11**, 511.

[30] N Tripathi, K Vijayarangamuthu and S Rath. A raman spectroscopic study of structural evolution of electrochemically deposited ZnO films with deposition time. *Mater. Chem. Phys.* 2011; **126**, 568-72.

[31] I Musa, N Qamhieh and ST Mahmoud. Synthesis and length dependent photoluminescence property of zinc oxide nanorods. *Results Phys.* 2017; **7**, 3552-6.

[32] JM Calleja and M Cardona. Resonant raman scattering in ZnO. *Phys. Rev. B* 1977; **16**, 3753.

[33] K Khun, ZH Ibupoto, MS AlSalhi, M Atif, AA Ansari and M Willander. Fabrication of well-aligned ZnO nanorods using a composite seed layer of ZnO nanoparticles and chitosan polymer. *Materials* 2013; **6**, 4361-74.